tvst

Article

Evaluation of Electrical Performance and Properties of Electroretinography Electrodes

Tony T. C. Man[1], Yolanda W. Y. Yip[1], Frederick K. F. Cheung[1], Wing Sze Lee[1], Chi Pui Pang[1], and Mårten Erik Brelén[1]

[1] Department of Ophthalmology and Visual Sciences, The Chinese University of Hong Kong, Kowloon, Hong Kong

Purpose: The aim of this study was to evaluate and compare the electrical performance and properties of commercially available electroretinography (ERG) electrodes.

Methods: A passive ionic model was used to measure impedance, noise, and potential drift in 10 types of ocular surface and skin ERG electrodes.

Results: The impedance for silver-based ocular electrodes are generally lower (range, 65.35–343.3 Ω) with smaller phase angles (range, −6.41° to −33.91°) than gold-based electrodes (impedance ranged from 285.95 Ω to 2.913 kΩ, and phase angle ranged from −59.65° to −70.01°). Silver-based ocular electrodes have less noise (median line noise of 6.48×10^4 nV^2/Hz) than gold-based electrodes (median line noise of 2.26×10^5 nV^2/Hz). Although silver-based electrodes usually achieve a drift rate less than 5 µV/s within 15 minutes, gold-base ocular electrode cannot achieve a stable potential. The exception is the RETeval strip type of silver electrode, which had an unusual drift at 20 minutes. The noise spectral density showed no change over time indicating that noise was not dependent on the stabilization of the electrode.

Conclusions: From the range of electrodes tested, lower impedance, lower capacitance, and lower noise was observed in silver-based electrodes. Stabilization of an electrode is effective against drift of the electrode potential difference but not the noise.

Translational Relevance: Application of electrodes with optimized materials improve the quality of clinical electrophysiology signals and efficiency of the recording.

Introduction

The electroretinogram (ERG) was discovered over 150 years ago by Holmgren, and it has since developed into a frequently used investigation for diagnosing a variety of retinal conditions.[1] Great advances have been made in the discovery of the ERG waveforms and their diagnostic relevance.

The electrode transducer serves as the interface between the subject and the biopotential recording system. High-quality electrodes with optimized electrical properties are crucial to obtaining a precise ERG recording. An ideal electrode should neither distort the signal nor impart additional noise, which requires low impedance, low capacitance, and low potential drift. This is particularly important for the ERG electrode because the signals are generally of low amplitude with low and narrow signal bandwidth.

The International Society for Clinical Electrophysiology in Vision (ISCEV) have clearly defined and are frequently updating the guidelines for performing electrodiagnostic tests. These publications have aimed to standardize the hardware, filter, and stimulation settings for full-field flash ERG,[2] pattern ERG,[3] multifocal ERG,[4] as well as visual evoked potential (VEP)[5] and electrooculogram (EOG).[6] The guidelines have unified the recording conditions, including specifying the preferred electrode contact impedance. It is well known that the amplitudes and signal to noise of the recorded signal can vary depending on the type of ERG electrode being used.[7–9] The current commercially available ERG electrodes vary in design and the materials used (see Supplementary Fig. S1),

translational vision science & technology

Table. ERG Electrodes Under the Study

Electrodes	Abbreviation	Metallic Material	Electrolyte
Ocular Electrode			
DTL Plus Electrode (Diagnosys LLC, Lowell, MA)	DTL	Silver	BSS
ERG-Jet (Fabrinal, La Chaux-de-Fonds, Switzerland)	JET	Gold	BSS
Burian-Allen Electrode Corneal electrode (Hansen Ophthalmic Development Lab, Coralville, IA)	BAC	Silver	BSS
Burian-Allen Electrode Palpebral Conjunctiva electrode (Hansen Ophthalmic Development Lab, Coralville, IA)	BAP	Silver	BSS
HK-Loop (Agencija Avanta d.o.o. Ljubljana, Ljubljana, Slovenia)	HKL	Silver	BSS
Gold Foil (UniMed Electrode Supplies, Farnham, Surrey, UK)	AUF	Gold	BSS
Skin Electrode			
Gold cup (Natus Manufacturing Limited, Gort, Co. Galway, Ireland)	AUC	Gold with silver bulk	Ten-20
Silver cup (Natus Manufacturing Limited, Gort, Co. Galway, Ireland)	AGC	Silver	Ten-20
Silver chloride cup (Technomed Europe, Maastricht, The Netherlands)	ACC	Silver-silver chloride	Ten-20
Red Dot 2249-50 (3M Health Care, St. Paul, MN)	RED	Silver-silver chloride	Pregelled
RETeval Sensor strip (LKC Technologies, Gaithersburg, MD)	LKC	Silver-silver chloride	Pregelled
Disposable disk electrode (Natus Neurology Incorporated, Middleton, WI)	NAT	Silver-silver chloride	Pregelled

however, there is little information in the literature comparing their electrical performance. Therefore the aim of this study was to compare the electrical characteristics of the most commonly available ERG electrodes. The objective properties that determine the electrode performance, including impedance, capacitance, noise, and potential drift, were investigated. These results will serve as a reference for clinicians and technicians when selecting a suitable electrode for their full-field flash, pattern, and multifocal ERG recordings.

Materials and Methods

Electrodes

There are broadly three categories of ERG electrodes commercially available: skin, conjunctival, and contact lens electrodes. The latter two electrodes for the purpose of this study are grouped together as ocular electrodes. In this study, five types of ocular electrodes and six types of skin electrodes are included. The names and materials of these electrodes are summarized in the Table. Pictures of the electrodes are provided in Supplementary Figure S1. Five electrodes were used during the recordings when testing the disposable electrodes, and the same electrode was testing five times when using non-disposable electrodes.

Electrolyte

Ten 20 electrolyte paste was used when testing the non-pregelled skin electrodes. For pregelled electrodes, there was no additional electrolyte required. Balanced salt solution (BSS) was applied to the ocular electrodes before testing to mimic the effect of tears, and BSS was reapplied frequently to keep the electrode well soaked during the experiment.

Passive Ionic Model

The experimental model previously reported by Tallgren et al.[10] was used in this study. In brief, flat blocks of agarose gel were prepared with physiological salt solution (Balanced Salt Solution; Alcon, Geneva, Switzerland) and 3% agarose (Certified Molecular Biology Agarose; BioRad, Hercules, CA). The electrodes were placed on top of the gel with their respective electrolyte applied. A good contact was ensured between the electrode and the agarose gel before the start of recording. For the corneal electrode that has a curved contact area, moderate pressure was applied until the metallic transducer came into contact with the gel. Motion artefacts were avoided by fixating the test electrodes firmly to the gel, and their cables were taped to the test bench using Micropore (3M Health Care, St. Paul, MN). The same reference electrode made of Ag/AgCl was used for all recordings and was applied on the agarose gel in the same manner as the test electrode. A schematic of the agarose gel setup is shown in Figure 1.

Impedance Measurement

Impedance recordings were made using an LCR meter (BK891 300 kHz Bench LCR meter; B&K Precision Corp., Yorba Linda, CA). The test electrodes were applied to the agarose gel for 30 minutes before the start, and the recordings were started to allow for stabilization. Data were exported and further analyzed in MATLAB (MathWorks, Inc., Natick, MA). Sweep recordings in the bandwidth of 20 Hz to 300 kHz
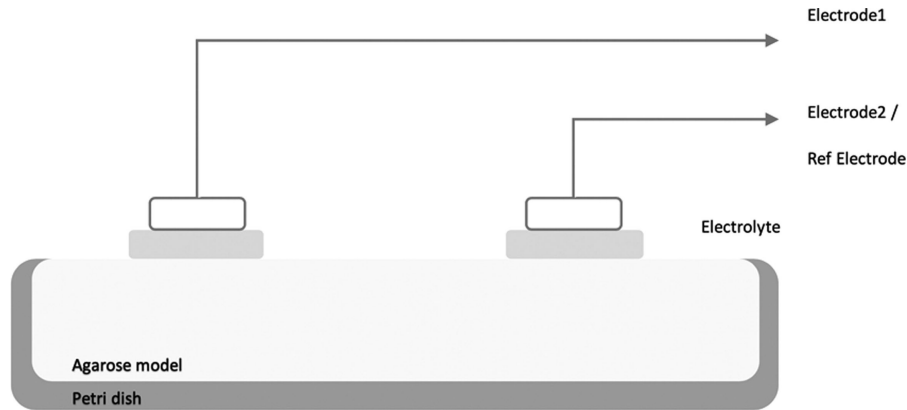
Figure 1. The passive ionic agarose gel model used for testing the electrodes. Electrode 1 is the test electrode and electrode 2 is the Ag/AgCl reference electrode. Electrolyte was applied between the electrode and agarose model and the electrodes securely fixated to avoid motion artefacts during recording.

were performed with 0.5 V root-mean-square amplitude. Five sweep recordings were made for each electrode. The frequency response of the impedance and phase angles (the electrodes capacitive properties) were analyzed in the bandwidth 20 Hz to 1 kHz. A separate analysis of the impedance and phase angle responses at 50 Hz was performed for each electrode. ERG signals can frequently be affected by 50 Hz power supply line noise, and hence this frequency response is of particular importance.

Noise and Potential Drift Measurement

The test electrode with its respective electrolyte and the reference electrode were placed on the agarose gel model as described earlier. Assuming no potential was being generated by the system, the signal recorded with this setup was considered as noise. Noise and potential difference were recorded using a clinical ophthalmic biopotential recording system (Diagnosys Espion E3 System; Diagnosys LLC, Lowell, MA). For these recordings there was no stabilization time prior to the recording. The background level of noise from the recording setup was also measured in a separate recording by shorting the two input leads, and this was used as the reference level during the signal analysis. Signals were filtered using Butterworth second order filter with a bandpass 0.001 to 500 Hz. Each recording session consisted of five sweep recordings with a 30-second interval between recordings.

The noise spectral density (NSD) is the noise power per unit of bandwidth. The MATLAB signal processing toolbox was used to perform the NSD calculation on our recorded signals. A separate analysis of the NSD at 50 Hz was also performed. For the potential drift measurements, an electrode was assumed to be stabi-

lized once the change in potential over time had fallen below 5 µV/s.

Data Process and Statistical Analysis

Collected data were stored and processed by MATLAB. The Wilcoxon rank-sum analysis was performed for comparison between the electrode groups, and Kruskal-Wallis analysis were performed for comparison between electrode impedance and NSD analysis. Bonferroni correction was applied to the multiple comparison following Kruskal-Wallis analysis.

Results

Impedance

The Bode impedance plot for ocular electrodes in the range of 20 Hz to 100 kHz is shown in Figure 2A. The area enclosed by the dotted box, from 20 to 300 Hz, indicates the impedance response within the ophthalmic signal frequency bandwidth. The gold ocular surface electrodes have significantly higher impedances. The impedance of the gold foil electrode ranged from 249.2 Ω to 1.966 kΩ in the bandwidth from 20 to 300 Hz. The impedance of the ERG-Jet electrode (Fabrinal, La Chaux-de-Fonds, Switzerland) was the highest with a range of 379.9 Ω to 2.842 kΩ, which is significantly more than the silver-based HK-Loop (Agencija Avanta d.o.o. Ljubljana, Ljubljana, Slovenia), which has a range between 144.9 and 193.3 Ω ($P < 0.0001$), and DTL Plus electrodes (Diagnosys LLC), which has a range between 65.35 and 99.79 Ω ($P < 0.0001$). For the
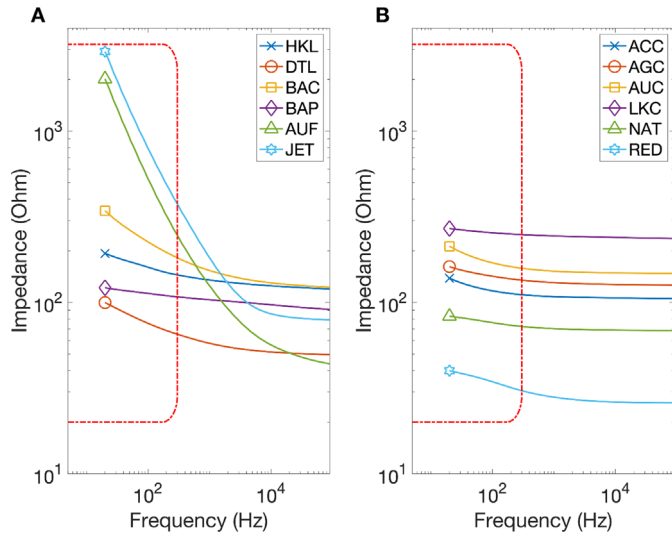
Figure 2. (A) Bode impedance plot for ocular electrodes. (B) Bode impedance plot for skin electrode. The dotted box encloses the frequency bandwidth of ophthalmic potentials. AUF, gold foil electrode; BAC, Burian-Allen corneal electrode; BAP, Burian-Allen palpebral conjunctival electrode; DTL, DTL Plus electrode; HKL, HK-Loop electrode; JET, ERG-Jet electrode; ACC, silver chloride cup electrode; AGC, silver cup electrode; AUC, gold cup electrode; LKC, RETeval sensor strip; NAT, disposable disk electrode; RED, RedDot 2249-50 electrode.
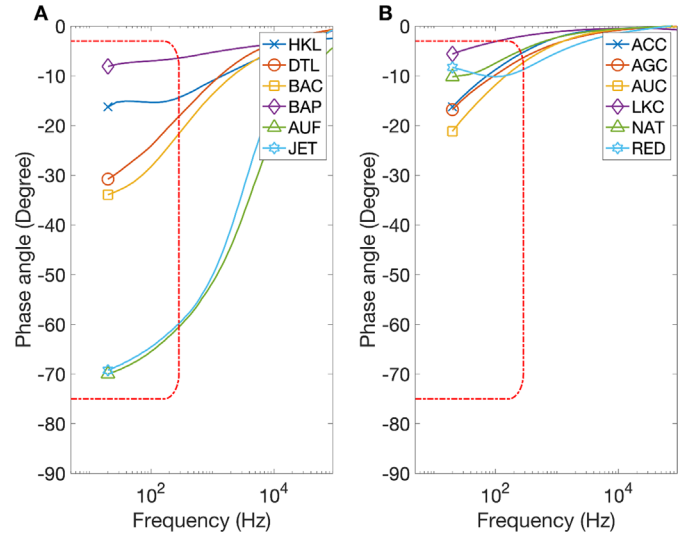
Figure 3. (A) Bode phase angle plot for ocular electrode. (B) Bode phase angle plot for skin electrode. The dotted box encloses the frequency band of ophthalmic potentials. AUF, gold foil electrode; BAC, Burian-Allen corneal electrode; BAP, Burian-Allen palpebral conjunctival electrode; DTL, DTL Plus electrode; HKL, HK-Loop electrode; JET, ERG-Jet electrode; ACC, silver chloride cup electrode; AGC, silver cup electrode; AUC, gold cup electrode; LKC, RETeval sensor strip; NAT, disposable disk electrode; RED, RedDot 2249-50 electrode.

Burian-Allen electrode (Hansen Ophthalmic Development Lab, Coralville, IA), both the corneal and the conjunctival electrodes have similar impedance to the silver-based electrodes. Impedances ranged from 182.8 to 343.3 Ω and 107.8 to 121.79 Ω for the Burian-Allen corneal and conjunctival electrode, respectively.

Significant differences were also found within the skin electrode group. As shown in Figure 2B, the silver chloride cup electrode (Technomed Europe, Maastricht, The Netherlands) had the lowest impedance within the non-pregelled electrode, with impedances ranging from 111.4 to 137.8 Ω. Such difference is significant against the gold cup electrode (Natus Manufacturing Ltd., Gort, Co. Galway, Ireland; $P < 0.0001$) but not against the silver cup electrode ($P = 0.1566$). For the pregelled electrodes, the RedDot electrode (3M Health Care) had the lowest impedance, with a range between 30.67 and 39.84 Ω. The highest impedance for the pregelled skin electrodes was found on the RETeval Strip (LKC Technologies, Gaithersburg, MD) with a range from 249.2 to 270.1 Ω. Differences between the pregelled electrodes were all significant ($P < 0.0001$).

The phase angle response of the ocular electrodes is shown in the Bode phase angle plot in Figure 3A. Silver-based electrodes have relatively small phase angles ranging from −18.14° to −30.66° for the DTL Plus electrode, and −14.35° to −16.23° for the HK-

Loop electrode. The two electrodes in the Burian-Allen had different phase angle properties, with the phase angle of the corneal electrode ranging from −21.61° to −33.91°, and the phase angle of the conjunctival electrode ranging from −6.41° to −8.09°. However, gold-based electrodes have large phase angles ranging from −60.52° to −70.01° for gold foil electrode (UniMed Electrode Supplies, Farnham, Surrey, UK), and −59.65° to −69.21° for ERG-Jet electrode. The differences between the phase angle responses of silver-based ocular electrodes and gold-based ocular electrodes are statistically significant ($P < 0.05$) with the exception of the gold foil electrode and the ERG-Jet electrode ($P = 0.0951$).

The phase angle response of skin electrodes is shown in Figure 3B. Phase angle responses of the silver chloride cup, silver cup (Natus Manufacturing Ltd.), and gold cup electrodes are −5.147° to −16.24°, −6.227° to −16.79°, and −7.057° to −21.13°, respectively. Again, the difference between the silver cup and silver chloride cup electrode was not significant. However, a significant difference was found between silver chloride cup electrode and gold cup electrodes ($P < 0.0001$). The pregelled electrodes have much smaller phase angle responses than the non-pregelled electrodes. The corresponding phase angles of the RETeval sensor strip, disposable disk electrode (Natus Neurology Incorporated, Middleton, WI), and
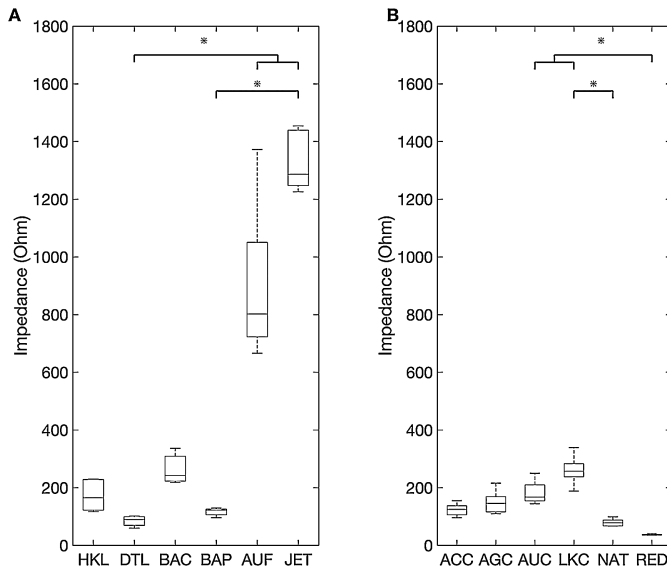
Figure 4. (A) Box plot of electrode impedances at 50 Hz for ocular electrodes; (B) Box plot of electrode impedances at 50 Hz for skin electrodes. RedDot 2249-50 electrode and DTL Plus electrode have the smallest and most stable impedance response among skin electrode and ocular electrodes, respectively. *Indicates significant difference (*P* < 0.05). AUF, gold foil electrode; BAC, Burian-Allen corneal electrode; BAP, Burian-Allen palpebral conjunctival electrode; DTL, DTL Plus electrode; HKL, HK-Loop electrode; JET, ERG-Jet electrode; ACC, silver chloride cup electrode; AGC, silver cup electrode; AUC, gold cup electrode; LKC, RETeval sensor strip; NAT, disposable disk electrode; RED, RedDot 2249-50 electrode.

RedDot electrode were −1.883° to −5.582°, −4.51° to −10.13°, and −8.277° to −10.15°, respectively. The differences between the phase angles response of skin electrodes are all statistically significant (*P* < 0.05), except between the silver chloride cup electrode and the silver cup electrode (*P* = 1), and between the gold cup electrode and the RedDot electrode (*P* = 0.3623).

The impedance response at 50 Hz was analyzed separately because ERG recordings can frequently be affected by power supply line noise. Figure 4A shows the box plot for 50 Hz impedance response of the ocular electrodes. The impedance response from the DTL Plus electrode (median 89.95 Ω, interquartile range [IQR] 69.01–99.10 Ω) and the Burian-Allen conjunctival electrode (median 122.06 Ω, IQR 106.25–125.525 Ω) was significantly lower than the gold-based electrodes, such as the gold foil electrode (median 801.91 Ω, IQR 723.21–1050 Ω; *P* < 0.0001) and the ERG-Jet electrode (median 1286.65 Ω, IQR 1247.32–1439.03 Ω; *P* < 0.0001). No significant difference was observed between the HK-Loop electrode (median 165.25 Ω, IQR 122.02–228.25 Ω), the Burian-Allen corneal electrode (median 242.36 Ω, IQR 222.41–308.72 Ω), and other ocular electrodes.

Figure 4B shows the equivalent box plot for the 50 Hz impedance responses of the skin electrodes. The mean electrode impedance were not significantly different between the non-pregelled silver chloride cup (median 126.7 Ω, IQR 105.92–137.37 Ω), the silver cup (median 145.72 Ω, IQR 116.07–167.87 Ω), and the gold cup (median 167.43 Ω, 154.43–209.5 Ω) electrodes. The RETeval strip electrodes showed the highest impedance, and the RETeval strip electrode (median 257.15 Ω, IQR 237.48–282.95 Ω) was significantly higher (*P* < 0.0001) than the disposable disk (median 78.48 Ω, IQR 67.83–87.63 Ω) and the RedDot electrodes (median 36.65 Ω, IQR 35.47–38.14 Ω).

Considering many areas have a power supply frequency of 60 Hz, impedance properties for the 60 Hz impedance response were evaluated as well. The difference in the impedances among the electrodes in 50 and 60 Hz was very similar, and thus not shown in the figure.

Noise Spectral Density

The NSD of the ocular electrodes are shown in Figure 5. Within the low-frequency range (1–10 Hz), median range of NSD for HK-Loop electrode (2.414×10^3 to 1.1×10^5 nV²/Hz), the DTL Plus electrode (1.838×10^3 to 6.974×10^4 nV²/Hz), the Burian-Allen conjunctival electrode (3.454×10^3 to 7.053×10^4) and the gold foil electrode (1.82×10^3 to 3.888×10^5 nV²/Hz) were similar with no significant differences. Signals recorded with the ERG-Jet electrodes and the Burian-Allen corneal electrode were significantly noisier (*P* < 0.0001) when comparing to all other ocular electrodes, with the range of median NSD from 1.096×10^4 to 1.426×10^7 nV²/Hz and from 1.539×10^5 to 4.808×10^8, respectively. The larger noise signal densities at lower frequencies indicates a more prominent baseline drift can be expected when using the ERG-Jet or the Burian-Allen corneal electrodes.

The NSD at 50 Hz power supply frequency can be seen as the prominent peak in Figure 5 (also indicated by the red dotted line). To better visual the difference in powerline noise, a box plot of powerline noise for the ocular electrodes is shown in Figure 6. Median NSD of the DTL Plus electrode and both Burian-Allen electrodes were found to be similar at the powerline frequency among the ocular electrodes. Signals recorded using these electrodes would expect a lower powerline noise. The skin electrodes did not show any additional NSD in low-frequency bandwidth or 50 Hz power supply frequency. The NSD of all skin electrodes were similar and showed no significant difference. The change of NSD showed no significant change over time
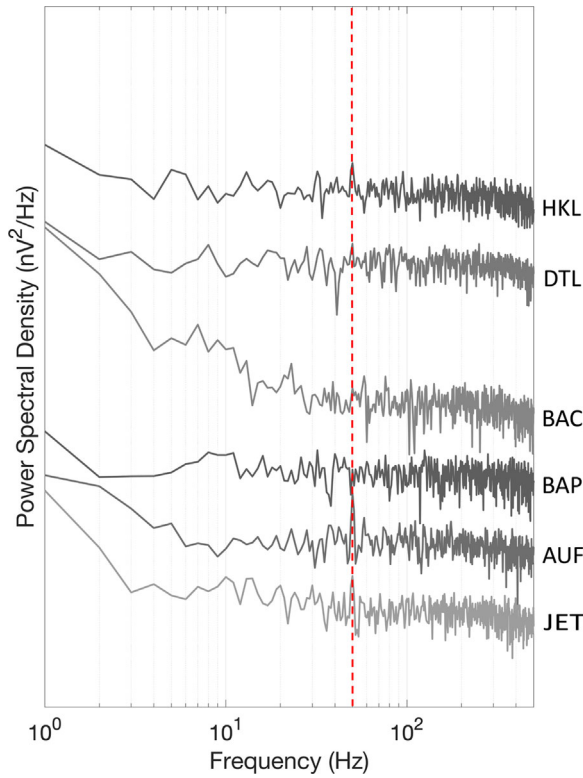
Figure 5. The NSD plot of ocular electrodes. Prominent differences can be observed in the low-frequency range (<10 Hz) between the electrodes and a peak is observed at 50 Hz as a result of power line noise interference. AUF, gold foil electrode; BAC, Burian-Allen corneal electrode; BAP, Burian-Allen palpebral conjunctival electrode; DTL, DTL Plus electrode; HKL, HK-Loop electrode; JET, ERG-Jet electrode. An offset of 10^x was used between traces.
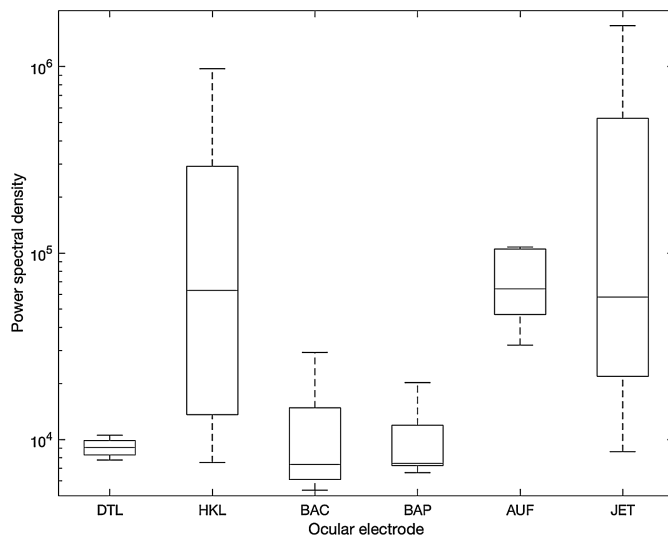

Figure 6. The box plot of the powerline NSD plot of ocular electrodes. Distribution of the noise density is coherent with the peak size in Figure 5. AUF, gold foil electrode; BAC, Burian-Allen corneal electrode; BAP, Burian-Allen palpebral conjunctival electrode; DTL, DTL Plus electrode; HKL, HK-Loop electrode; JET, ERG-Jet electrode.

Figure 7. (A) Potential drift (μV/s) against time of the ocular electrodes. The potential difference between ERG-Jet electrode and reference electrode remained unstable for the entire 60-minute recording interval. Most of the silver-based electrodes stabilized much faster than gold-based electrodes. (B) Potential drift (μV/s) against time for the skin electrodes. AUF, gold foil electrode; BAC, Burian-Allen corneal electrode; BAP, Burian-Allen palpebral conjunctival electrode; DTL, DTL Pl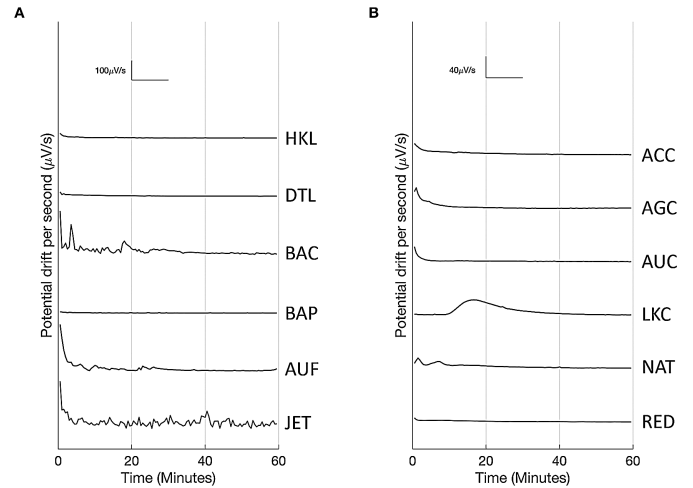us electrode; HKL, HK-Loop electrode; JET, ERG-Jet electrode; ACC, silver chloride cup electrode; AGC, silver cup electrode; AUC, gold cup electrode; LKC, RETeval sensor strip; NAT, disposable disk electrode; RED, RedDot 2249-50. An offset of 10^x was used between traces.

indicating that the stabilization of electrodes did not have any effect on noise performance.

Potential Drift

Figure 7A shows the potential drift of ocular electrodes during a 60-minute recording period. The ocular electrodes stabilized over time but with variable rate. The potential drift of the gold-based electrode, including the gold foil electrode and the ERG-Jet electrode, were the most unstable. The drift fluctuated during the entire 60 minutes of recording and never settled below 5μV/s. The Burian-Allen corneal electrode also showed fluctuating potential drift at the beginning, and eventually stabilized after 35 minutes. Generally, the silver-based electrodes stabilized faster. The median time required for the DTL Plus electrode, the HK-Loop electrode, and the Burian-Allen conjunctival electrode to stabilize were 13, 6, and 2.5 minutes, respectively. Toward the last 10 minutes of recording, the potential drift had reduced even further to 1.235 and 1.673 μV/s. Figure 7B shows the potential drift over time for skin electrodes. Overall, the drift in potential among skin electrodes is less than that of ocular electrodes and they showed a more rapid stabilization. For the non-pregelled skin electrode, the

median stabilization time of the silver cup electrode, the silver chloride cup electrode, and the gold cup electrode were 15, 9.5, and 4.335 minutes, respectively. For the pregelled skin electrode, the median stabilization time of the disposable disk electrode and the RedDot electrode were 21.5 and 1.5 minutes, respectively. The stabilization for the RETeval strip electrode followed an unusual trend. On repeated measurement, the drift was found to increase during the first 20 minutes and then stabilized slowly toward the end of 60 minutes. Deformation of the electrolyte gel was also seen during the recording session, which may have contributed to the potential drift recording.

Discussion

The Resistive and Capacitive Characteristics of Electrode Impedance

The simplified model reported by Geddes et al.[11] used a resistive and capacitive parallel circuit and is suitable for modeling the ophthalmic electrodes evaluated in this study. The resistive component allows the net flow of charge across the electrode-electrolyte interface,[12] which mainly represents the redox reaction taking place on the electrode surface. The capacitive component is formed by multiple frequency-dependent effects, including capacitive coupling.[13] Although no electrode is purely resistive nor purely capacitive, they can be described by the dominance of a resistance or capacitance effect. As reported in previous studies, the behavior of an electrode is highly dependent on the redox reaction between the metal and the electrolyte.[14] For electrodes composed of reactive metals, the corresponding electrode is usually more resistive, and for inert metals, the electrode tends to be more capacitive.

The capacitive properties of the electrodes can be measured by the Bode phase angle plot. The silver-based ocular electrodes used in ophthalmic recording tend to have a small phase lag and are subsequently more resistive in nature. However, the phase lag of the gold-based ocular electrodes is higher, and these electrodes have a dominant capacitive component. As inert metals, gold is less reactive than silver. It is therefore less involved in the redox reaction across the electrode-electrolyte interface. This explains the strongly capacitive effect of this non-faradaic metal. Out of all gold-based electrodes, the gold cup used in this study showed the lowest phase angles, and therefore the least capacitive response.

Interaction Between Signal and Electrode Impedance

In a capacitive electrode, charge accumulates on either side of the electrode, and thereby establishes a potential difference across the interface. The generated electric field and the charge exchange process can be described by the displacement current, which is highly dependent on the electrode-electrolyte interface. Therefore capacitive electrodes are more vulnerable to motion artefacts than resistive electrodes. This explains why signals recorded by the gold-based ocular electrodes tend to be more unstable (Fig. 6) and have more drift (Fig. 7).

The effect of power line noise interference in electrical recordings is well known and has been described in numerous previous publications.[15,16] The amplitude of capacitive coupled noise is determined by both induction current amplitude and electrode impedance, therefore greater power noise interference is expected from electrodes that have high impedance at power supply frequency. As can be seen in Figure 6, it is observed that the gold foil and ERG-Jet electrodes will be more vulnerable to power supply interference. Out of the skin electrodes, the greatest impedance at 50 Hz was found in the RETeval strip electrode.

Reliability of Performance

The ocular electrodes were generally more unstable than skin electrodes. Without proper fixation and a steady supply of electrolyte, severe distortions could be seen during the recordings. Overall, we found the DTL Plus electrode was the most stable in terms of impedance and noise response among the ocular electrodes.

Skin electrodes were generally more stable than the ocular electrodes with the most stable performance found in the RedDot electrode. The electrolytes of skin electrode are either in gel or paste form and this helped to stabilize the electrode on the agarose gel. The improved stability together with the electrolyte not drying out improved the repeatability of the recordings and reduced the drift.

Noise from Electrode Electrolyte Interface

The noise from the electrode-electrolyte interface has been shown to be incomparable with amplifier noise.[17] In this study, we found that the NSD was similar to the level generated by the amplifier, suggesting that any additional noise introduced by the use of skin electrodes from the electrode-electrolyte interface was generally negligible. However, for ocular electrodes

there is a significant difference in the NSD observed within the low-frequency range. Therefore the choice of ocular electrodes can have a significant effect on the noise in ERG recordings. A prominent density peak is observed in all electrodes at the power supply frequency (50 Hz), which occurs due to capacitive coupling. Those electrodes with lower impedance had a smaller NSD at 50 Hz. In general, the silver-based electrodes with smaller capacitive responses also have lower NSD, especially at 50 Hz.

Influence of Potential Difference Drift Across the Input Electrodes

The potential drift of an electrode is defined as the change in potential across the test and reference electrode over time (µV/s). The two half-cells in the corresponding differential input will form an electrochemical cell, the potential difference of which is determined by the imbalance between the half-cell potentials. This potential is influenced by various environmental factors that generate an inevitable potential drift across the two input leads.[18] Besides, the amplitude of the potential difference drift depends on the standing potential across the electrode pair, which is also in turn affected by the impedance response between the electrode-electrolyte interface. As the exchange of charge across the interface for resistive electrodes is more reactive, the potential difference across the electrode can be quickly equalized, and thus there is less polarization and lower drift. This drift is usually a slow changing potential and attenuated by bandpass filtering of the signal. However, even with DC rejection (by using an AC coupled amplifier or bandpass filtering), the potential drift can still affect recorded signals. This is often observed in recordings as a slow-moving baseline recording drift, which makes the measurement of amplitudes more difficult. Our results show a greater drift in the gold-based electrodes, which is coherent with the results from impedance testing, as the gold-based electrodes are more capacitive than the silver-based electrodes. They are therefore expected to give a worse performance when recording ERG in patients.

The results from this study have demonstrated the large variability in performance of electrodes used in ERG recordings and also indicate further improvements can be made in ERG electrode design. Ultimately, an electrode with low impedance, low capacitance, and low drift should be used on our patients. However, further studies are needed to determine the effect that different materials might have on clinical ERG recordings.

Effect of Electrical Performance and Electrode Recording Performance

In this study, the performance of ERG electrodes were compared, and silver-based electrodes were found to have lower impedance, lower noise, and lowest drift. Although some skin electrodes have shown comparable performance, and even better stability, the recording of ERG using skin electrodes is affected by many other factors. First, the remote location of the electrode from the source of the signal attenuates the signal. Second, the ion-insulating skin can introduce additional noise and attenuate signals further. Finally, skin electrodes require skin surface treatment, which leads to variability from one recording session to the next. With all these factors in mind, the recorded signals from skin electrodes are generally worse, with lower signal to noise ratio as compared with ocular electrodes. Line noise, high electrode impedance, and drift are common problems clinicians face when recording ERGs. Line noise is the result of the interaction between induced current from capacitive coupling and impedance from the electrode-electrolyte interface. As shown in our results, impedance from the electrode-electrolyte interface of silver electrodes were generally smaller than those of gold electrodes. As the amount of induced current is independent of the material in the electrode, it is anticipated less line noise will be recorded when using silver-based electrodes. The spectral density plot in our study also indicate that less noise was observed among silver-based electrodes. Additional means, such as shielding and signal-preamplification, can provide more protection against line noise interference by reducing the induced current from capacitive coupling. For the optimum reduction in line noise, the use of a silver-based electrode with preamplification is recommended.

Conclusions

From the range of electrodes tested, lower impedance, lower capacitance, and lower noise was observed in silver-based electrodes. Stabilization of an electrode is effective against drift of the electrode potential difference but not the noise.

Acknowledgments

References

1. Perlman I. The electroretinogram: ERG. In: Kolb H, Fernandez E, Nelson R, eds. *Webvision: The Organisation of the Retina and the Visual System*. Salt Lake City: University of Utah Health Sciences Center; 2007.
2. McCulloch DL, Marmor MF, Brigell MG, et al. ISCEV standard for full-field clinical electroretinography (2015 update). *Doc Ophthalmol*. 2015;130:1–12.
3. Bach M, Brigell MG, Hawlina M, et al. ISCEV standard for clinical pattern electroretinography (PERG): 2012 update. *Doc Ophthalmol*. 2013;126:1–7.
4. Hood DC, Bach M, Brigell M, et al. ISCEV standard for clinical multifocal electroretinography (mfERG) (2011 edition). *Doc Ophthalmol*. 2012;124:1–13.
5. Odom JV, Bach M, Brigell M, et al. ISCEV standard for clinical visual evoked potentials: (2016 update). *Doc Ophthalmol*. 2016;133:1–9.
6. Constable PA, Bach M, Frishman LJ, Jeffrey BG, Robson AG, International Society for Clinical Electrophysiology of V. ISCEV standard for clinical electro-oculography (2017 update). *Doc Ophthalmol*. 2017;134:1–9.
7. Carpi F, Benini G, Tomei F, Figliuzzi RM, De Napoli A. Electroretinographic wet electrode. *Med Eng Phys*. 2009;31:923–929.
8. Bayer AU, Mittag T, Cook P, Brodie SE, Podos SM, Maag KP. Comparisons of the amplitude size and the reproducibility of three different electrodes to record the corneal flash electroretinogram in rodents. *Doc Ophthalmol*. 1999;98:233–246.
9. Barber C. Electrodes and the recording of the human electroretinogram (ERG). *Int J Psychophysiol*. 1994;16:131–136.
10. Tallgren P, Vanhatalo S, Kaila K, Voipio J. Evaluation of commercially available electrodes and gels for recording of slow EEG potentials. *Clin Neurophysiol*. 2005;116:799–806.
11. Geddes LA, Roeder R. Measurement of the direct-current (Faradic) resistance of the electrode-electrolyte interface for commonly used electrode materials. *Ann Biomed Eng*. 2001;29:181–186.
12. Weinman J, Mahler J. An analysis of electrical properties of metal electrodes. *Med Electron Biol Eng*. 1964;2:299–310.
13. Ragheb T, Geddes LA. The polarization impedance of common electrode metals operated at low current density. *Ann Biomed Eng*. 1991;19:151–163.
14. Feder W. Silver-silver chloride electrode as a nonpolarizable bioelectorde. *J Appl Physiol*. 1963;18:397–401.
15. Huhta JC, Webster JG. 60-HZ interference in electrocardiography. *IEEE Trans Biomed Eng*. 1973;20:91–101.
16. Metting van Rijn AC, Peper A, Grimbergen CA. High-quality recording of bioelectric events. Part 1. Interference reduction, theory and practice. *Med Biol Eng Comput*. 1990;28:389–397.
17. Huigen E, Peper A, Grimbergen CA. Investigation into the origin of the noise of surface electrodes. *Med Biol Eng Comput*. 2002;40:332–338.
18. Aronson S, Geddes LA. Electrode potential stability. *IEEE Trans Biomed Eng*. 1985;32:987–988.

translational vision science & technology